

ADVERSE REYNOLDS NUMBER EFFECT ON MAXIMUM LIFT OF TWO DIMENSIONAL AIRFOILS

Kenji YOSHIDA, Masayoshi NOGUCHI
Advanced Technology Aircraft Project Center
NATIONAL AEROSPACE LABORATORY
6-13-1 Osawa, Mitaka, Tokyo 181-0015 JAPAN

Keywords: *transition, short bubble, turbulent separation, NACA 8318, wind tunnel test*

Abstract

An adverse Reynolds number effect on C_{lmax} of NACA 8318 airfoil was experimentally investigated, using a rectangular wing model with an aspect ratio of 5.7. At a little lower Reynolds number than that of old test data by NACA, a slight decrease of the C_{lmax} , namely the adverse effect was confirmed. Furthermore, short bubble that did not play a major role in the old explanation given by Tani was also observed at the condition showing the adverse effect. The adverse effect is clearly based on the forward movement of turbulent separation point, and we assumed new mechanism that the forward movement was dominated by the initial state of turbulent boundary layer at reattachment point.

At relatively higher Reynolds numbers, large adverse effect was also obtained and it strongly originated in three-dimensionality of separated flow. This means such three-dimensionality is more important in the study on C_{lmax} of two-dimensional airfoils in addition to the new mechanism, because turbulent separation has almost three-dimensionality at high Reynolds numbers.

1 Introduction

In the aerodynamic design of aircrafts, the estimation of high Reynolds number effect on maximum lift (C_{lmax}) from wind tunnel test results is very important. We generally expect the C_{lmax} increases with an increase in Reynolds number. But recently some results on the

decrease of C_{lmax} were experimentally observed [1, 2]. This phenomenon is called "adverse Reynolds number effect" or "adverse effect". Its mechanism is qualitatively explained as follows [1]. In a simple swept wing, transition due to attachment-line contamination occurs near the leading edge at high Reynolds numbers. This means that turbulent boundary layer on the upper surface grows from the stagnation point. In this situation, the C_{lmax} generally decreases. The swept wing has usually local maximum section lift (C_l) at about 70 to 80% semi-spanwise station. If that maximum local C_l decreases, the total lift (C_L) also decreases. However, Ref.1 has never given any method predicting the adverse effect. Therefore, any detail study is necessary.

By the way, such an adverse effect had already been observed on special two-dimensional airfoils such as NACA 8318 and 9324 airfoils [3, 4]. In general, Reynolds number effect on behavior of the C_{lmax} of a two-dimensional airfoil is explained as follows [5]. At low Reynolds numbers, the C_{lmax} is nearly constant, because the C_{lmax} is mainly dominated by laminar separation which is independent on Reynolds numbers according to a boundary layer theory. As the Reynolds number increases, the laminar-separated flow reattaches on the surface and a laminar separation bubble is formed. Therefore the angle of attack to keep an attached flow near the leading edge increases, and then the C_{lmax} rapidly increases. As the Reynolds number increases further, natural transition is caused before the laminar

separation occurs. In usual airfoils with a not-so-large camber and thickness, the transition nearly occurs at suction peak. Since an increase of Reynolds number reduces turbulent boundary layer thickness, the reduction of a circulation due to viscous effect is relaxed. Consequently the C_{lmax} slightly increases.

On the other hand, in some airfoils such as NACA 8318 airfoil with a large camber and thickness, the adverse pressure gradient after the suction peak is not strong even at a high angle of attack. Therefore, natural transition is located fairly downstream from the suction peak point. If the Reynolds number increases, the transition point moves forward to the suction peak point. Since the turbulent boundary layer on the upper surface is thickened in this situation, the circulation is reduced. Consequently, this effect leads to a slight decrease of the C_{lmax} .

This mechanism is different from that in the swept wing as mentioned above, but it is common that the relative relation between transition and separation is essence of determining the maximum lift. Although the above explanation was given by Tani about a half century ago [5], there were few studies on the adverse effect except Ref.4. Therefore, as a first step to advance such a study of Reynolds number effect on maximum lift of three-dimensional wings, we have paid attention to the behavior of the C_{lmax} on two-dimensional airfoils. The purpose of present study is to understand the mechanism of adverse effect in detail and to develop a method predicting the behavior of the C_{lmax} at high Reynolds numbers.

Some years ago, one of authors conducted numerical and experimental studies [6] to confirm the Tani's explanation. We found that it was not valid in our test Reynolds number range, and pointed out that short bubble also played a major role in adverse effect. Then we recently conducted an improved wind tunnel test to investigate our new consideration on the adverse effect.

In this paper, first of all, a brief summary of our previous work is given in section 2 as a background. Next some results of present work on the improved wind tunnel test and its

analysis are described in section 3. Finally a conclusion and future work are mentioned in section 4 as a summary in our study.

2 Previous Work

2.1 Numerical Study

First of all, we first investigated Tani's explanation on 40 NACA 4-digit airfoils, using a potential flow theory, a boundary layer theory and an empirical transition prediction method. In the numerical result on NACA 8318, we confirmed the forward movement of natural transition with an increase in Reynolds number as explained by Tani. Then we summarized the relations of minimum pressure, laminar separation and transition locations in the following two categories. The first type corresponds to the NACA 8318; the second type has no features similar to the first one.

When comparing them with experimental results and having some rough assumptions, we made a criterion on judging whether or not an airfoil showed an adverse effect as shown in Fig.1. Using this figure, we can approximately predict that some airfoils in the shadow region show the adverse effect. For example, NACA 6212 airfoil with $(f/c, x_m/c, t/c)=(6\%, 20\%, 12\%)$ is chosen as a typical airfoil showing the adverse effect [6].

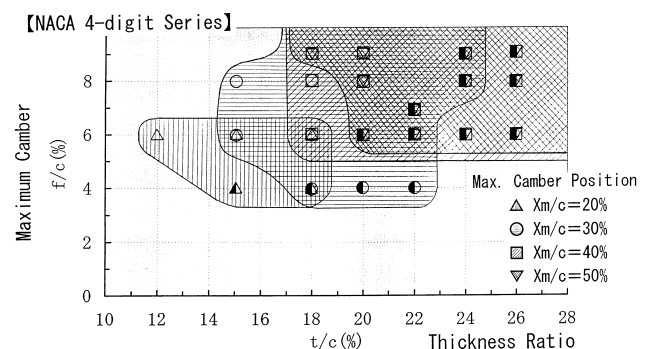


Figure 1 A criterion on judging an airfoil with an adverse Reynolds number effect

2.2 Experimental Study

We have two objectives in our experimental study. The first one is to check whether or not

the NACA 6212 airfoil shows an adverse effect. The second one is to confirm the forward movement of transition as pointed out by Tani. To perform these objectives, we used a rectangular wing model with two large end-plates shown in Fig.2 to realize a two dimensional flow condition. From force and pressure measurement tests, we were able to achieve the first objective as shown in Fig.3.

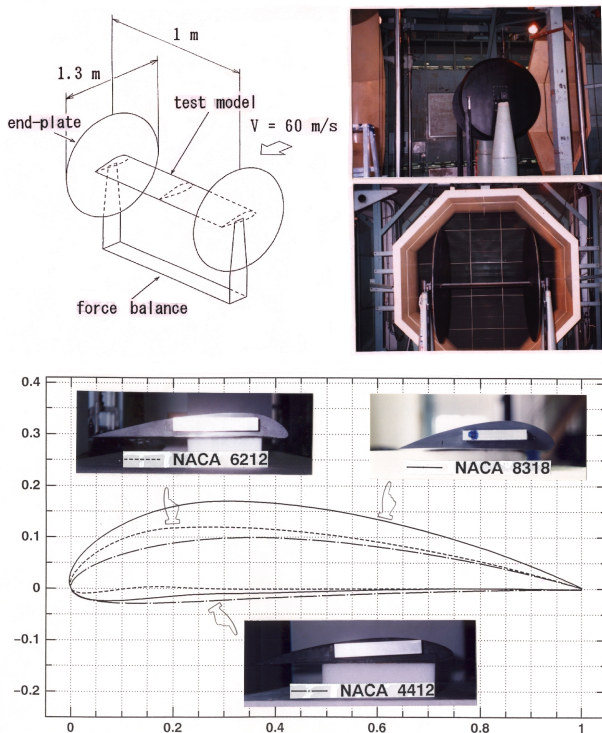


Figure 2 Wind tunnel test models and set-up

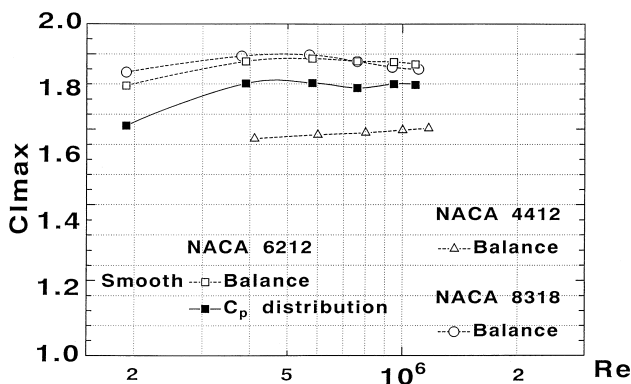


Figure 3 Experimental results on Reynolds number characteristics of C_{lmax}

Next we conducted flow visualization test using liquid crystal film for the second

objective. We obtained not a natural transition point but a reattachment point $(x/c)_{R.A.}$, because we observed a short bubble at the whole range of our test Reynolds numbers. In the behavior of $(x/c)_{R.A.}$ summarized in Fig.4, we found that there were two trends in the movement (Type I and II), and the Type II trend was related to the condition showing an adverse effect.

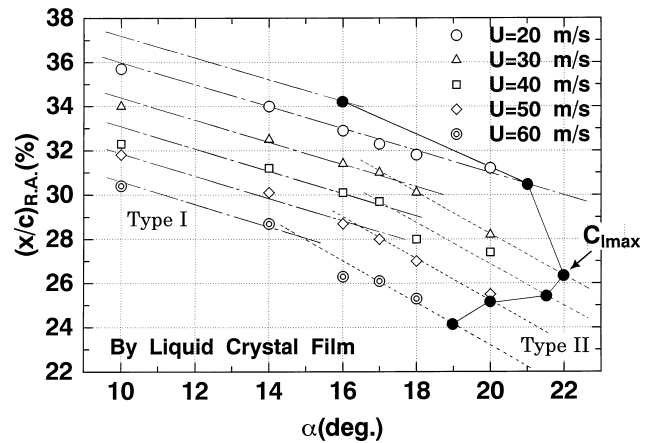


Figure 4 Behavior of observed reattachment point on NACA 8318

2.3 Consideration on the Mechanism of Adverse Reynolds Number Effect

Based on our experimental results, we summarized Reynolds number effect on C_{lmax} as follows: We think there are three factors dominating the growth of turbulent boundary layer. 1) The growth rate is always reduced with an increase in Reynolds number. 2) The forward movement of $(x/c)_{R.A.}$ increases the length of turbulent boundary layer. If a short bubble doesn't exist, and the second factor is more dominant than the first one, an adverse effect certainly is caused. This corresponds to Tani's explanation, but the existence of a short bubble leads to the third factor: 3) the quality of initial turbulent boundary layer starting from $(x/c)_{R.A.}$.

Since the Type II trend is observed under the condition of relatively higher Reynolds numbers and angles of attack, we consider the quality to be very bad, namely higher shape factor, due to the strong entrainment process for reattachment. Therefore, as the third factor promotes the effect of second one, we predict the forward movement of turbulent separation.

On the other hand, since the Type I trend corresponds to relatively lower Reynolds numbers and angles of attack, the quality is not so bad. Therefore, the third factor promotes the effect of first one, and we predict the rearward movement of turbulent separation.

2.4 Summary

We had the following conclusions: 1) Tani's explanation is not valid in our test Reynolds number range, but it is probably valid if natural transition occurs at higher Reynolds numbers before laminar separation. 2) Our criterion is approximately useful. 3) The mechanism of adverse effect is essentially based on the forward movement of turbulent separation. It is dominated by the quality of initial state of turbulent boundary layer.

However, we also had some problems as follows: 1) to investigate the influence of the end-plates, 2) to confirm the existence of a short bubble at higher test Reynolds numbers, 3) to validate our explanation for the mechanism of an adverse effect mentioned above.

3 Present Work

3.1 Outline of Improved Wind Tunnel Test on NACA 8318 Airfoil

As one of trials to solve those problems, we recently conducted an improved wind tunnel test using a new wing model with a larger aspect ratio than that of previous test. The set-up of the model in NAL gust wind tunnel (GWT) facility is shown in Fig.5. (It was not operated at any gust condition.) Spanwise and chordwise length of the model is 2m and 0.35m respectively. Since its aspect ratio is about 5.7 comparing with about 3.3 in the previous model, we can expect better two-dimensional flow condition.

The main objectives of this test are to confirm an adverse effect more clearly and to prove the existence of a short bubble at the condition showing the adverse effect. To perform these objectives, we measured pressure distribution at more chordwise points and investigated laminar separation, transition and

reattachment points in detail, using Preston tube and China clay technique. Furthermore, we also performed flow visualization by a lot of tufts to obtain flow pattern of separated region.



Figure 5 New test model with tufts for flow visualization in NAL gust wind tunnel

3.2 Some Results of Improved Wind Tunnel Test

3.2.1 Lift Coefficient and Pressure Distribution

Figure 6 shows the relation between obtained C_{lmax} and Reynolds number based on its chordwise length (Re_c). We found a slight decrease in the range from $Re_c=0.38$ to 0.75 million and a large decrease beyond $Re_c=7.5$ million. Although we confirmed the adverse effect, this behavior was very different from the result by NACA.

Figure 7 shows typical lift curves at some Reynolds number conditions, and each arrow symbol indicates maximum point. Those lift curves almost reflect so-called trailing edge stall type, but a slight change of the stall pattern between $Re_c=0.75$ and 0.87 million was also found. The change seems to relate to the large decrease of C_{lmax} as mentioned above.

ADVERSE REYNOLDS NUMBER EFFECT ON MAXIMUM LIFT OF TWO DIMENSIONAL AIRFOILS

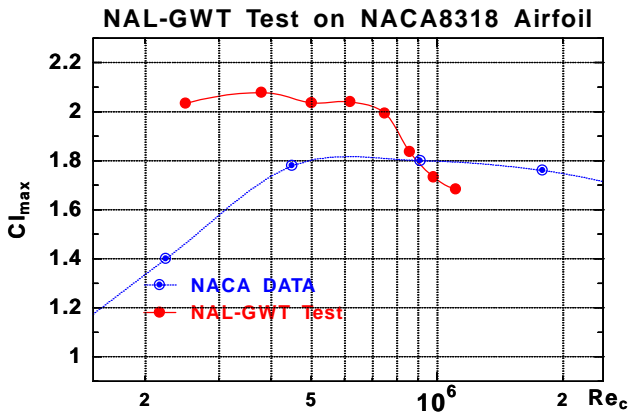


Figure 6 Improved test result of Reynolds number effect on the C_{lmax} of NACA 8318

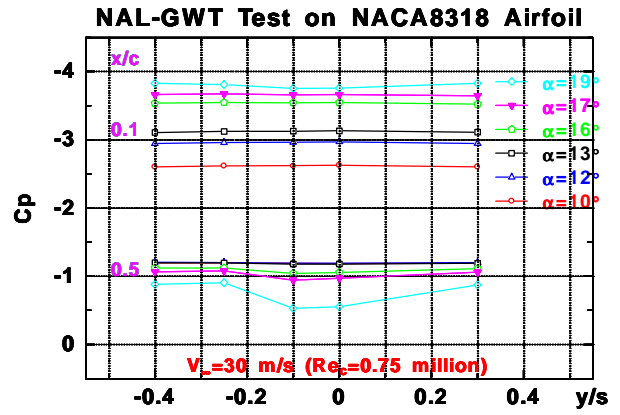


Figure 8(b) Spanwise pressure distribution at $Re_c=0.75$ million

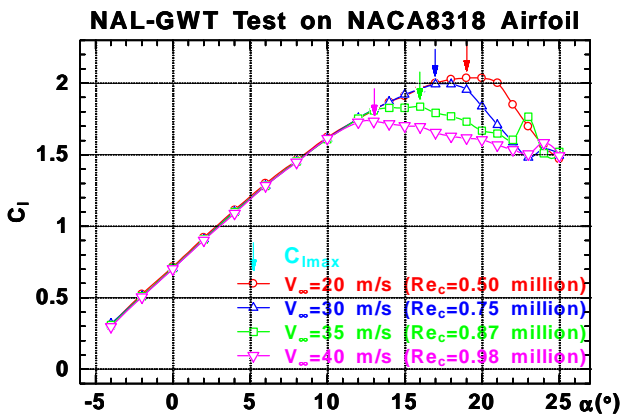


Figure 7 Lift characteristics

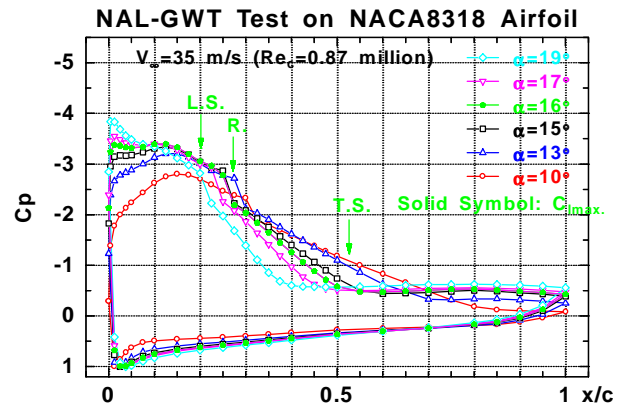


Figure 9(a) Chordwise pressure distribution at $Re_c=0.87$ million

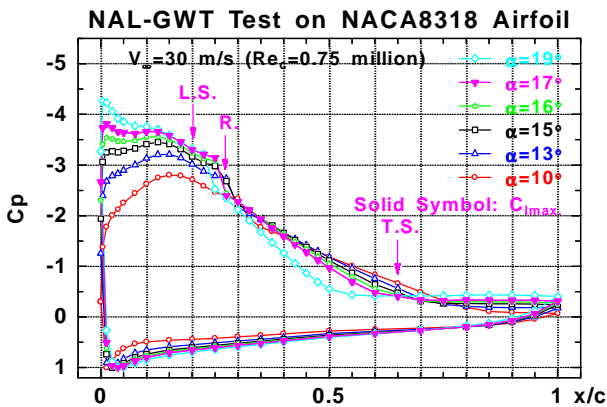


Figure 8(a) Chordwise pressure distribution at $Re_c=0.75$ million

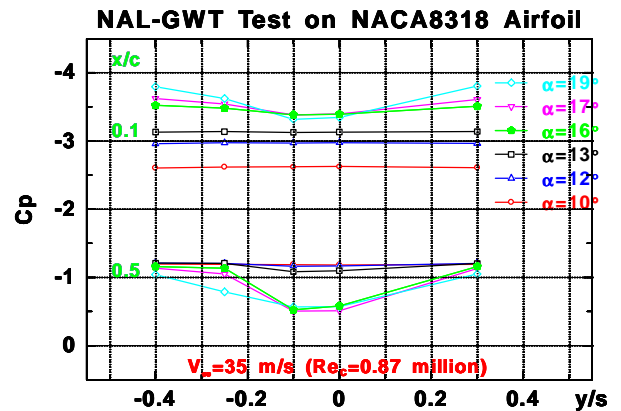


Figure 9(b) Spanwise pressure distribution at $Re_c=0.87$ million

Figures 8 and 9 show chordwise and spanwise pressure distributions at several angles of attack (α) and $Re_c=0.75$ and 0.87 million respectively. Solid symbols show the pressure distributions at $C_{l,max}$. The symbols of L.S., R. and T.S. mean a laminar separation point, a reattachment point and a turbulent separation point respectively, which were qualitatively estimated through physical consideration of the shape of pressure distributions. In those figures, we confirmed the existence of a short bubble clearly, and found two dimensionality of flow-field at $C_{l,max}$ condition below $Re_c=0.75$ million. However, three-dimensionality appeared at $Re_c=0.87$ million.

Figure 10 shows chordwise pressure distributions at $\alpha=16$ and 19 degrees and various freestream velocity (V) conditions. These angles correspond to the $C_{l,max}$ at $V=35\text{m/s}$ and 20m/s . At $\alpha=19$ degrees, there is little difference on the pressure distributions between $V=20\text{m/s}$ and 30m/s , except the region from short bubble to turbulent separation point. Reynolds number effect is mainly seen in this region. As V increases to 30m/s , the short bubble length decreases as well known and the separation point moves forward. The latter leads to a slight decrease of $C_{l,max}$. Although it is different from usual Reynolds number effect, we assume it relates to the short bubble. This result is the same as previous test one.

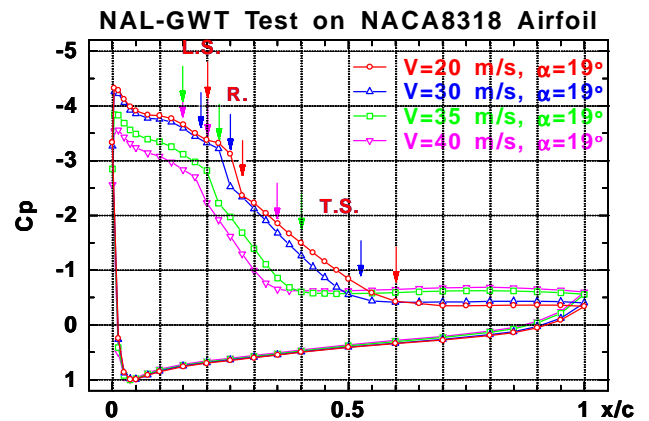


Figure 10(b) Chordwise pressure distribution at $\alpha=19$ degrees

At both $\alpha=16$ and 19 degrees, there is large difference on the pressure distributions between $V=30\text{m/s}$ and 35m/s . The difference at $\alpha=16$ degrees reflects the large decrease of $C_{l,max}$. Therefore, we assume this phenomenon is dominated by the three-dimensionality of separated flow as well as the Reynolds number effect on a short bubble, because the difference is too large.

3.2.2 Separated Flow Pattern

To investigate the three-dimensionality of separated flow in detail, we conducted a flow visualization test using lots of tufts put on the surface. Figure 11 is one of typical test results.

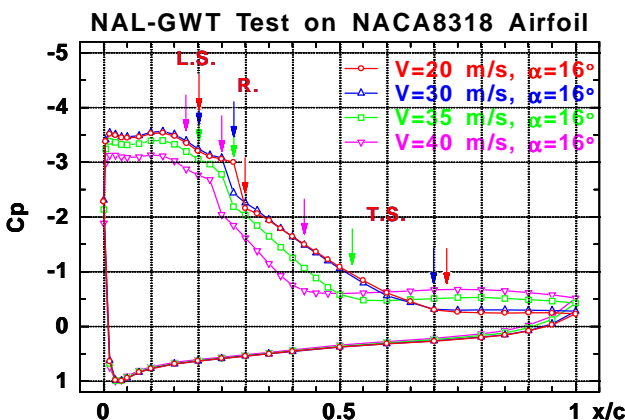


Figure 10(a) Chordwise pressure distribution at $\alpha=16$ degrees

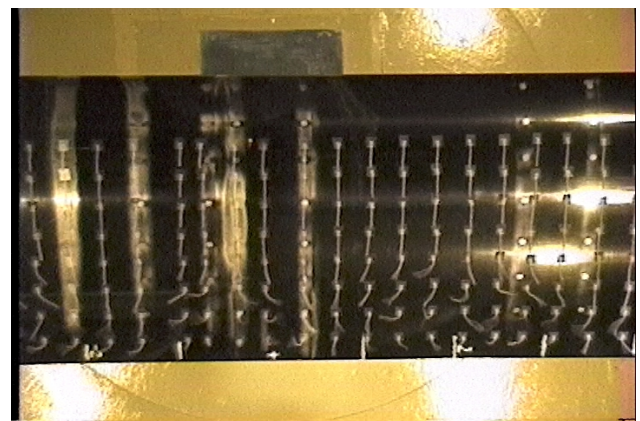


Figure 11 Tuft test result at $V=40$ m/s ($Re_c=0.98$ million) and $\alpha=12$ degrees

Figure 12 shows sketches based on the test results. At the condition of $V=30\text{m/s}$, we found that a separated flow region approximately kept two dimensionality near stall. On the other hand, at $V=40\text{m/s}$, the separated flow region indicated three-dimensionality. Therefore, according to present results on pressure measurement and flow visualization tests, we assumed that present strong adverse Reynolds number effect above $Re_c=0.75$ million was dominated by the three-dimensionality of separated region.

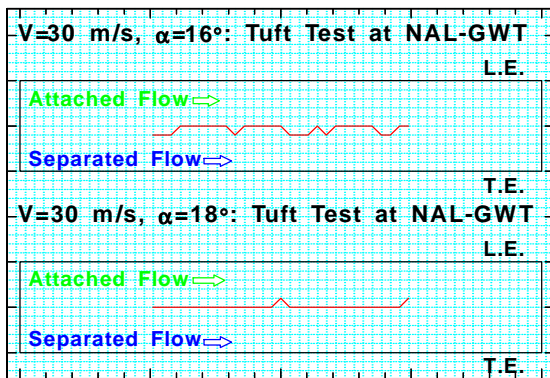


Figure 12(a) Sketches on tuft test result at $V=30\text{m/s}$ ($Re_c=0.75$ million) just below and above stall angle

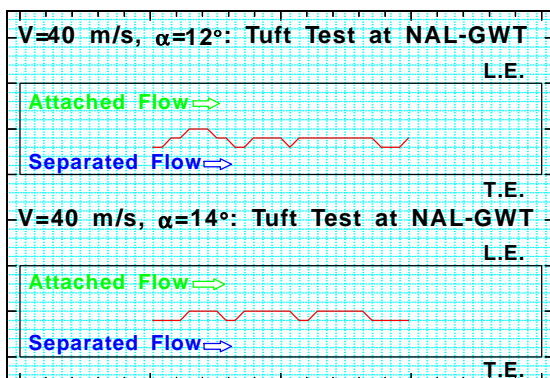


Figure 12(b) Sketches on tuft test result at $V=40\text{m/s}$ ($Re_c=0.98$ million) just below and above stall angle

3.2.3 Information on short bubble

To obtain more detail information on a short bubble, first we measured total pressure change within boundary layer at several angles of attack and chordwise positions, using three Preston tubes put on the surface as shown in Fig.13. Then, we estimated both locations of onset and end of transition (T.) in the bubble, based on the measurement data.



Figure 13 Preston tubes put on the surface

Figure 14 shows boundary layer characteristics indicated by the symbols of L.S., R. and T.S. The end location of transition almost coincides with the reattachment location based on the pressure distribution. And we found that the onset location of transition existed within the bubble and near the reattachment location. This means transition region in the bubble is very narrow. Therefore we confirmed reattachment phenomenon was dominated by strong entrainment process. (In both figures, numerical results as mentioned later are also shown as a reference.)

Next we performed flow visualization to investigate the bubble length, applying a China clay technique. Figure 15 is one of test results. Based on those data, the locations on laminar separation and reattachment were summarized in Fig.14. We found there was almost good agreement between China clay and pressure measurement tests. Therefore, we also clearly confirmed the existence of a short bubble at $C_{l,max}$ condition.

3.3 Numerical Analysis of Improved Wind Tunnel Test Results

To investigate the influence of initial state of turbulent boundary layer, we analyzed boundary layer characteristics of the test results. As a first step, we interpolated a measured pressure distribution by a smooth curve except a short bubble region, using a Fourier series expansion technique. Figure 16 shows a typical result.

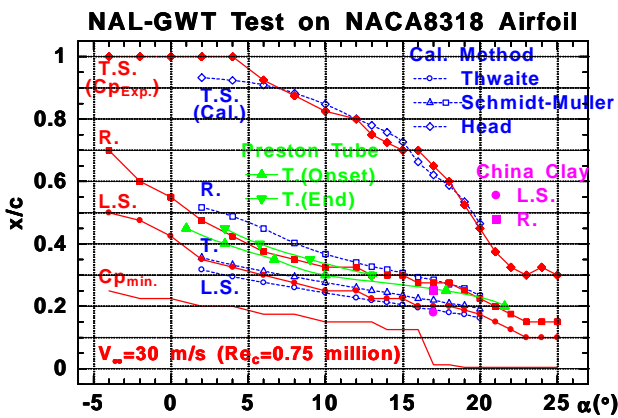


Figure 14(a) Boundary layer characteristics at $V=30$ m/s ($Re_c=0.75$ million)

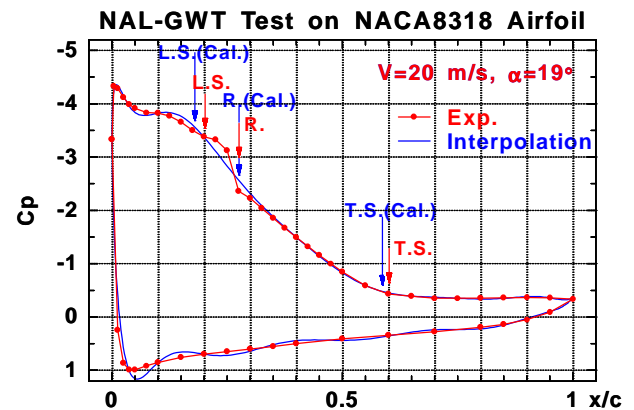


Figure 16 Comparison of measured and interpolated pressure distributions

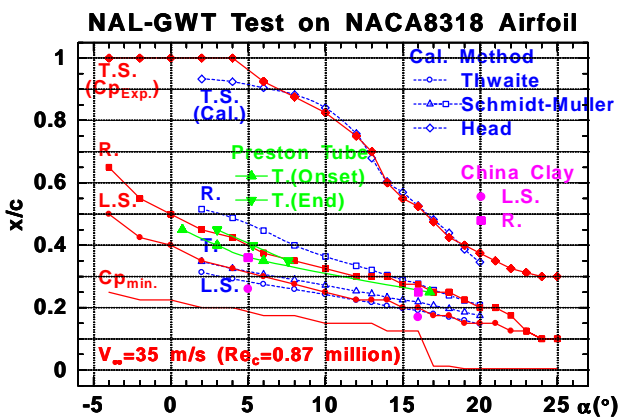


Figure 14(b) Boundary layer characteristics at $V=35$ m/s ($Re_c=0.87$ million)



Figure 15 Flow visualization result by China clay technique at $V=40$ m/s and $\alpha=10$ degrees

Based on the interpolated pressure distributions, we estimated (1) a laminar separation point by Thwaite method [7], (2) a reattachment point by Schmidt-Mueller's short bubble model [8] and (3) a turbulent separation point by Head method [7]. To simulate the test results in this approach, we slightly modified the formulation of Schmidt-Mueller model (see Appendix) and made the following assumption: turbulent separation occurred at the position where shape factor (H) reached to maximum. Some results of present analysis are summarized in Fig.14 comparing with test results. Since good agreement was obtained above $\alpha=10$ degrees, we tried to investigate the influence of initial state of turbulent boundary layer.

Figure 17 shows estimated shape factors at reattachment point (H_R) and turbulent separation point ($H_{T.S.}$) respectively. First of all, all $H_{T.S.}$ have the values between 1.8 and 2.4. In usual Head method, turbulent separation occurs at the condition of $H=1.8$ to 2.2. This selection

is based on the rapid increase of H near the separation, but the interpolated pressure distribution has never strong recovery toward trailing edge because of the existence of turbulent separation. Therefore, since the shape factor generally decreases through the maximum value, we changed the separation criterion on the shape factor into the assumption as mentioned above.

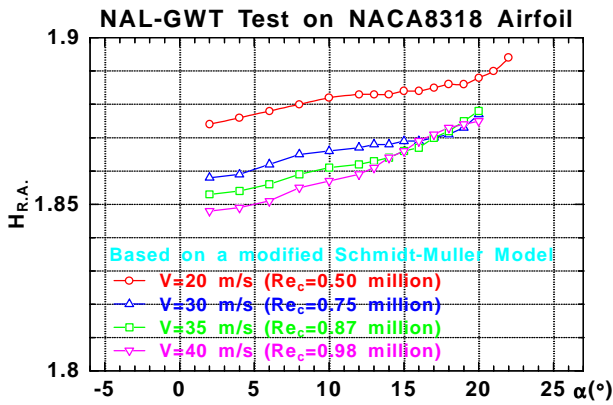


Figure 17(a) Estimated shape factor distributions at reattachment point

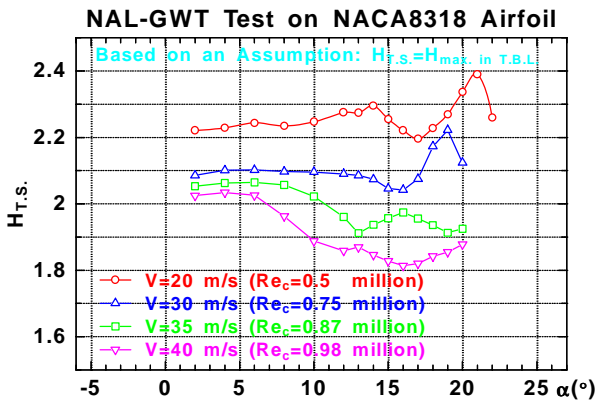


Figure 17(b) Estimated shape factor distributions at turbulent separation point

On the other hand, all H_R have the values between 1.84 and 1.9. This means all cases have “bad” quality as initial state of turbulent boundary layer. In the Schmidt-Mueller model, the initial shape factor (H_0), namely H_R , decreases as Reynolds number increases. This feature is opposite to our consideration on the

mechanism of an adverse effect in the previous work. Therefore, to analyze the influence, we conducted a parametric study on the initial shape factor. Figure 18 shows the result on estimated chordwise H distributions. However, we found no remarkable movement of turbulent separation point corresponding to each H_0 artificially changed. If this analysis is valid, we will find the change of H_0 has little influence on the movement of turbulent separation point. However, since the Schmidt-Mueller model was not derived taking into account such an adverse effect, any further study will be necessary to clear the mechanism.

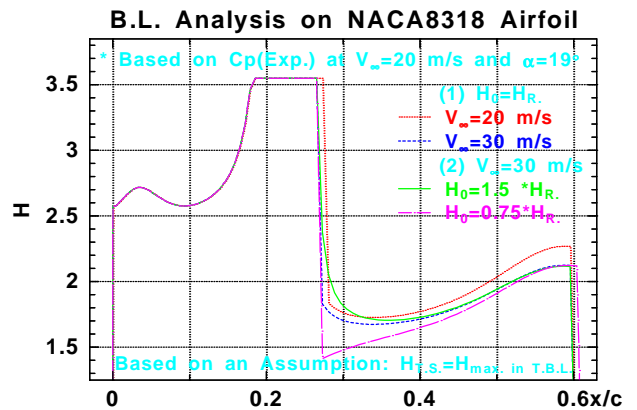


Figure 18 Result of parametric study on the influence of initial shape factor

3.4 Consideration of three-dimensionality

Although the large decrease of $C_{l,max}$ was observed at relatively higher Reynolds numbers, we assumed that this was based on the three-dimensionality of turbulent separation as mentioned above. The main reason for the large three-dimensionality is as follows. Although a wing with high aspect ratio has strong two-dimensionality, turbulent separation always generates three-dimensionality due to its unsteadiness. In general, local three-dimensional separation has a trend to localize own separated region due to the interference of its outer and separated flows. If such local three-dimensionality occurs on the wing with strong two-dimensionality, the three-dimensional feature would become more remarkable.

However if the same situation occurs on the wing with weak three-dimensionality of outer flow such as the influence of a lower aspect ratio wing tip, it would have a possibility of suppressing the three-dimensionality of separated flow by the three-dimensionality of outer flow. We think it corresponds to our previous test.

Therefore, to investigate Reynolds number effect on $C_{f,max}$ in detail, we have to reconsider all test results on two-dimensional airfoils very carefully, namely two-dimensionality of their separated flow. We are now planning such a study, considering some tests on the models with different aspect ratio will be effective. And we expect to obtain any information on the influence of initial shape factor after the study.

4 Concluding Remarks

Main conclusions are summarized as follows.

- 1) An adverse effect which consists of a slight decrease of the $C_{f,max}$ of NACA 8318 airfoil was experimentally confirmed at relatively lower Reynolds number than that of old test data by NACA.
- 2) Since a short bubble was clearly observed at the condition showing the adverse effect, Tani's explanation is not enough to understand its mechanism. Therefore, we assumed other mechanism that the initial state of turbulent boundary layer at reattachment played a major role on the movement of turbulent separation point.
- 3) We obtained good agreement with test results in predicting boundary layer characteristics including a short bubble, by modifying Schmidt-Mueller short bubble model and assuming a new criterion on turbulent separation.
- 4) However, our new mechanism of an adverse effect has not been validated yet experimentally and numerically.
- 5) Large adverse effect was also observed at relatively higher Reynolds numbers and it strongly originated in three-dimensionality of separated flow. Since turbulent separation has almost three-dimensionality at high Reynolds numbers, such three-dimensionality is more

important even in the study on the $C_{f,max}$ of two-dimensional airfoils.

References

- [1] Hardy B. C. Experimental investigation of attachment-Line transition in low-speed, high-lift wind tunnel testing, *AGARD-CP-438*, 2-1, 1989.
- [2] Mack M. D. and McMasters J.H. High Reynolds number testing in support of transonic airplane development, *AIAA Paper 92-3982*, 1992.
- [3] Jacobs E. N. and Sherman A. Airfoil section characteristics as affected by variations of the Reynolds number, *NACA Report*, No.586, 1936.
- [4] Kamiya N., et al. Some practical aspects of the burst of laminar separation bubbles, *ICAS-80-10.2*, 1980.
- [5] Tani I. *Applied fluid dynamics*, Iwanami Course, Physics, p.81, 1940 (In Japanese).
- [6] Yoshida K. and Ogoshi H. Study for Reynolds number effect on $C_{f,max}$ of 2-dimensional airfoils, *ICAS-96-3.1.2*, 1996.
- [7] Cebeci T. and P. Bradshaw, *Momentum Transfer in Boundary Layers*, 1977
- [8] Schmidt, G. and Mueller, T.J. Analysis of Low Reynolds Number Separation Bubble Using Semiempirical Methods, *AIAA J.*, Vol.27, No.8, pp.993-1001, 1989

Appendix. Modification of Schmidt-Mueller's Short Bubble Model

In the original Schmidt-Mueller's short bubble model, the following relation is used to estimate a reattachment point [8]:

$$\Lambda_R \equiv \left(\frac{\theta}{U} \frac{dU}{dx} \right)_R = -0.0082$$

Here a subscript R means the value at the reattachment. By the way, to obtain good agreement with our test result, we found modification of $\Lambda_R = -0.003$ was effective.

In addition, since any information on the initial value of shape factor (H) is necessary to calculate turbulent boundary layer using Head method, we used the following well-known relation.

$$H_R = 3.0 - \Delta H$$

$$\Delta H = 0.35 + 0.3875 \log_{10}(R_{\theta_R}) - 0.0375 (\log_{10} R_{\theta_R})^2$$

Here R_{θ} means a Reynolds number based on momentum thickness.